Wind Over San Francsico Bay and the Sacramento-San Joaquin River Delta: Forcing for Hydrodynamic Models

Allie King
San Francisco Estuary Institute

March 25, 2019

1 Introduction

The Ludwig wind model (Ludwig et al., 1991; Ludwig and Sinton, 2000) has been used to generate spaio-temporally varying wind inputs for hydrodynamic models of the San Francisco Bay and Sacramento-San Joaquin River Delta (SFB-Delta) in recent projects at Deltares (Achete et al., 2015), at the United States Geological Survey (USGS; Martyr-Koller et al., 2017), and at San Francisco Esturary Institute (SFEI; Nuss et al., 2018). These projects all utilize hydrodynamic models in the Deltares suite of software known as DFlow (e.g., Deltares, 2019), and the wind inputs to DFlow are specified hourly on a 1.5 km x 1.5 km grid.

The Ludwig wind model interpolates wind observations in a manner informed by terrain and vertical temperature stratification: in the presence of weak stratification, wind will go over hills, and in the presence of strong stratification, wind will go around hills. The model requires input data in a very specific format, and it is not trivial to translate wind observations into this format. Presently, a server at the Oakland Air Route Traffic Control Center in Fremont, CA collects real-time wind and meteorological data from over fifty stations around the SFB-Delta as well as vertical profiles from a weather balloon in Oakland, and writes these data to text files in the Ludwig model input format. These text files are uploaded to the website of Professor Douglas Sinton at San Jose State University where they are archived and made available to the public: **http://www.met.sjsu.edu/∼sinton/winds**. Scientists working on the DFlow projects at Deltares, USGS, and SFEI download the Ludwig input files from Professor Sinton's website and run the Ludwig model (compiled from Fortran source code) locally, using in-house Matlab/Python scripts to read the binary output of the Ludwig model and write it to DFlow wind input files in the proper format. Our

investigations revealed that Deltares and SFEI use slightly different versions of the Ludwig model, but the results are nearly identical. Although we do not have a copy of the version of the Ludwig model used by USGS in the Martyr-Koller et al. (2017) paper, it appears to be a third version, but again the results are nearly identical to the results of the other two versions.

This report details our effort to validate the DFlow wind inputs generated by the Ludwig model, and our effort to develop a new method to generate wind inputs for DFlow (and potentially other hydrodynamic models) that is simpler than the Ludwig model and does not entail a chain of events across multiple institutions between the wind observations and the hydrodynamic model wind input files. It happens that our new method for generating wind fields is more accurate than the Ludwig model across the SFB-Delta and nearby coastal ocean.

We have developed a package called **SFEI_Wind** that contains:

1. wind/meteorological observation data from 52 stations around the SFB-Delta, downloaded from ASOS, CIMIS, and NDBC networks,

2. a Python script to estimate hourly 10-m wind vectors from the station observation data and compile the hourly 10-m wind vectors into a consolidated dataset that is easy to use,

3. a Python script for generating DFlow wind input files (*.amu/*.amv) from the consolidated hourly 10-m wind data set, using either linear or natural neighbor interpolation,

4. a Python script for validating DFlow wind input files (*.amu/*.amv) by comparing to observed wind at the 47 stations within the wind input domain, and

5. a Python script for validating the linear and natural neighbor interpolation methods by excluding one of the 47 wind observation stations at a time from the input data before interpolating and comparing interpolated hourly 10-m winds to observed 10-m winds at the excluded station.

The **SFEI_Wind** package is available on SFEI's Google Drive via the following link: **https://bit.ly/2U54rNZ**. Contact Allie King at **alliek@sfei.org** with questions. At this time, DFlow wind input files for WY2001-WY2017, generated using the natural neighbor interpolation method, are available in the **Wind4DFlow-SFB** directory of the **SFEI_Wind** package.

Note that throughout this report, we refer often to "water year" or "WY". In the SFB-Delta region, "water year N" or "WYN" conventionally refers to the period between October

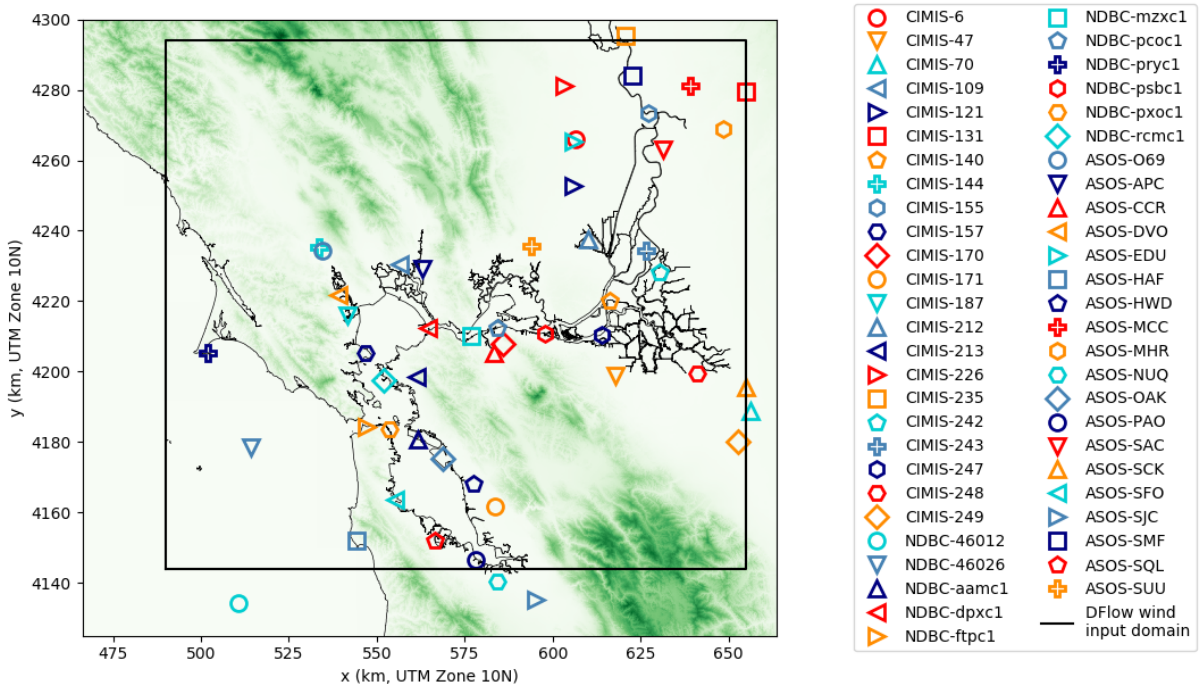

Figure 1: This map shows the locations of the 52 wind observation stations used to compile the SFEI hourly 10-m wind data set. Terrain is plotted in green (SFB 90-m DEM, 2011), and the boundary of the DFlow wind input grid is plotted as a black rectangle.

1 of year $(N-1)$ and September 30 of year N. In this report, "water year N" or "WYN" technically refers to the period between August 1 of year $(N-1)$ and September 30 of year N. This is because two extra months are included in hydrodynamic model inputs to allow the model to warm up.

2 Wind Observation Data

For the purposes of validation and generating new wind inputs, we compile wind observation data from 52 stations around the SFB-Delta. Only stations near the water and in flat areas have been included, since these should best correlate with winds over the water surface. The 52 stations are plotted in Figure 1 along with terrain, the SFB-Delta shoreline, and the boundary of the DFlow wind input grid. Note that 47 of the 52 stations are inside the DFlow wind input grid domain. Stations belong to three observation networks: the Automated Surface Observing System (ASOS), the California Irrigation Management Information System (CIMIS), and the National Data Buoy Center (NDBC). The URL's for these three networks, from which wind and auxiliary meterological data are downloaded, are listed in Table 1.

Table 1: URL's for ASOS, CIMIS, and NDBC wind observation networks.

Network	URL
ASOS	**https://mesonet.agron.iastate.edu/request/download.phtml**
CIMIS	**https://cimis.water.ca.gov/WSNReportCriteria.aspx**
NDBC	**https://www.ndbc.noaa.gov**

The ASOS network primarily operates wind measurement stations at airports. Anemometers are located at 10-m height, ideally, though actual height may be either 27 ft (8.2 m) or 33 ft (10.1 m) depending on local regulations. We do not know which stations have anemometers at which heights. Wind measurements at ASOS stations are averaged over 2-minute intervals and reported at the end of the averaging interval. The reporting interval varies by station and, to some degree, also over time. In Table 2, we show latitude/longitude as well as reporting interval (in early 2017) for each ASOS station included in our wind data set.

Table 2: Station information for ASOS wind observation stations included in our data set. Reporting interval, $\Delta T_{rep.}$, varies over time for some ASOS stations, e.g., it may be one hour in 2010 and five minutes in 2017. The values of $\Delta T_{rep.}$ reported here are for early 2017.

Station	Latitude	Longitude	$\Delta T_{rep.}$
APC	38.2075	-122.2804	5.0 min
CCR	37.9916	-122.0526	5.0 min
DVO	38.1436	-122.5561	20.0 min
EDU	38.5315	-121.7865	20.0 min
HAF	37.5136	-122.4996	20.0 min
HWD	37.6588	-122.1212	5.0 min
MCC	38.6670	-121.4006	20.0 min
MHR	38.5553	-121.2973	1.0+ hr
NUQ	37.4059	-122.0490	5.0 min
O69	38.2578	-122.6053	20.0 min
OAK	37.7213	-122.2207	5.0 min
PAO	37.4611	-122.1151	1.0+ hr
SAC	38.5069	-121.4950	5.0 min
SCK	37.8942	-121.2383	5.0 min
SFO	37.6190	-122.3749	5.0 min
SJC	37.3594	-121.9244	5.0 min
SMF	38.6954	-121.5908	5.0 min
SQL	37.5119	-122.2483	20.0 min
SUU	38.2627	-121.9275	$\sim$1.0 hr

CIMIS stations are ideally located in flat, grassy, areas where the grass is mowed to three inches (7.6 cm). CIMIS anemometers are located at height $z_a = 2.0$ m. Air temperature,

relative humidity, and soil temperature are also measured at CIMIS stations – the height of the air temperature sensors is $z_t = 1.5$ m, and the height of the humidity sensors is $z_q = 1.5$ m. CIMIS data is averaged over hourly time intervals and reported at the end of each hourly interval. The latitude and longitude of each CIMIS station included in our data set is listed in Table 3.

Table 3: Locations of the CIMIS wind observation stations included in our wind data set.

Station	Latitude	Longitude
6	38.5357	-121.7764
47	37.9283	-121.6599
70	37.8348	-121.2232
109	38.2195	-122.3550
121	38.4156	-121.7869
131	38.6500	-121.2189
140	38.1217	-121.6745
144	38.2664	-122.6165
155	38.5992	-121.5404
157	37.9955	-122.4677
170	38.0154	-122.0203
171	37.5988	-122.0532
187	38.0909	-122.5267
212	38.2781	-121.7411
213	37.9315	-122.3027
226	38.6727	-121.8117
235	38.7979	-121.6114
242	38.1924	-121.5103
243	38.2496	-121.5555
247	38.0334	-121.7012
248	37.9321	-121.3967
249	37.7556	-121.2662

The NDBC does not operate all of the stations included in its data network. Although the NDBC does operate some meterological stations located on buoys, much of the data on its website comes from meterological stations operated by other agencies and entities. Many of these stations are located at the ends of docks extending from shore or on bridges over the water. None of the NDBC stations we have included in our data set are on land. The NDBC website provides some information about stations in its network, including anemometer height, z_a, temperature sensor height, z_q, and the time interval over which continuous wind data is averaged to obtain the reported measurement, $\Delta T_{avg.}$. We have tabulated this information, along with station location and reporting interval, $\Delta T_{rep.}$ (inferred from the data sets), in Table 4 for NDBC stations in our data set. Several NDBC stations for which critical information (e.g., anemometer height) was not available were excluded from our data

set even though they met the criteria of being on flat terrain near water.

Table 4: NDBC wind observation station information. ΔT_{avg} is the period over which continuous wind measurements are averaged before reporting, $\Delta T_{rep.}$ is the reporting interval, z_a is anemometer height, and z_t is temperature sensor height. For NDBC stations located on the shoreline, typically on docks, the sensor heights reported here are the heights above the water.

Station	Latitude	Longitude	$\Delta T_{avg.}$	$\Delta T_{rep.}$	z_a	z_t
46012	37.356	-122.881	8.0 min	1.0 hr	5.0 m	4.0 m
46026	37.754	-122.839	10.0 min	1.0 hr	4.0 m	4.0 m
aamc1	37.772	-122.300	2.0 min	6.0 min	10.4 m	7.7 m
dpxc1	38.056	-122.264	2.0 min	6.0 min	7.6 m	3.4 m
ftpc1	37.806	-122.466	2.0 min	6.0 min	10. m	9.0 m
mzxc1	38.035	-122.125	2.0 min	6.0 min	10.5 m	7.8 m
pcoc1	38.056	-122.039	2.0 min	6.0 min	11.2 m	10.5 m
pryc1	37.996	-122.977	2.0 min	6.0 min	8.7 m	7.9 m
psbc1	38.040	-121.887	2.0 min	6.0 min	7.6 m	3.4 m
pxoc1	37.798	-122.393	2.0 min	6.0 min	16.2 m	15.6 m
rcmc1	37.923	-122.410	2.0 min	6.0 min	10.0 m	9.2 m

3 Processing of Wind Observation Data

Ideally, all wind data would be measured at 10-m height and averaged over 10-minute intervals, since this is the standard upon which reported drag coefficients are based in most literature. 10 minutes is a nice compromise between turbulent time scales (which tend to be much less than 10 minutes) and longer-term variability of wind due to shifting forcing factors. Wind averaged over longer intervals (e.g., hourly) will exhibit less variability (e.g., smaller standard deviation) compared to 10-minute data, and vice-versa for wind averaged over shorter intervals (e.g., 2 mintutes).

The wind observation stations in our data set utilize a wide variety of averaging intervals (2 minutes to 1 hour) and reporting intervals (6 minutes to 1 hour), as reported in Tables 2-4. Only one station utilizes a 10 minute averaging interval. In the interest of standardization, we have chosen to average all of the wind and auxiliary meteorologcial measurements in our data set onto a uniform hourly time axis. One hour is the shortest time interval we could chose, since the CIMIS data represents hourly averages already. Note that we use a vector average for winds. Before averaging wind and other meterological variables onto the hourly time axis, we remove outliers by computing the mean μ, and standard deviation, σ for each year, based on the wind vector components, and eliminating measurements with vector components outside the $\mu + / - 3\sigma$ window.

Users of our wind input files should keep in mind that we have used hourly averages and consider increasing drag coefficients or using a wind multiplication factor to account for the discrepency from 10-minute winds. Users should also keep in mind that some of the ASOS wind data, which represent 2-minute averages, are reported hourly or at times even less frequently, and in such cases "hourly average" may be the average of just one 2-minute average wind data point. Two of the NDBC stations similiarly average data over short time intervals but report hourly.

After the wind and auxiliary meterological data are averaged onto a uniform hourly time axis, we estimate the 10 m wind speed using the COARE 3.6 algorithm (Fairall et al., 2018). This algorithm estimates wind speed at 10 m from wind speed, air temperature, water temperature, and humidity measured at specified heights, using the Monin-Obukhov stability parameter to account for the effects of temperature stratification on the velocity profile, and estimating surface roughness from wind speed (and optionally wave age and wave height).

We downloaded the COARE 3.6 algorithm from the following FTP site:
ftp://ftp1.esrl.noaa.gov/BLO/Air-Sea/bulkalg/cor3_6/ and translated the original Matlab scripts into Python. In addition to translating into Python, we modified the COARE

3.6 algorithm in the following ways:

1. eliminated most of the outputs, so only 10-m wind speed is output,

2. eliminated the "jcool" option, which estimates skin temperature from near-surface water temperature measurements, since this option requries measurements of shortwave and longwave radiation that we do not have at our wind observation stations,

3. eliminated the option to include wave height and age in estimates of surface roughness since this option also requires measurements we don't have, and

4. added the option to handle wind stations on land. To activate the over-land option, the user must input the roughness lengths for momentum, temperature, and humidity. In the default case of flow over water, these are estimated from wind speed.

Since the ASOS observation stations directly measure wind at 10 m, we only use the modified COARE 3.6 alogrithm for NDBC and CIMIS stations. For CIMIS stations, which are on land, we specify roughness lengths of $z_0 = 0.023$ m for momentum, $z_{0,t} = 0.0023$ m for temperature, and $z_{0,q} = 0.0023$ m for humidity, following recommendations by Brutsaert (1982) and Hignett (1994) for grassy areas mowed to 10 cm (assuming the 7.6 cm grass grows out a bit between mowings). Note that detailed information about specific CIMIS sites is available at **https://cimis.water.ca.gov/Stations.aspx**, and future versions of **SFEI_Wind** could potentially take into account the details of each site in estimates of roughness lengths, but this is not the case now. Since humidity is not measured at the NDBC stations, we use a default relative humidity of 85% for these stations, as suggested on the NDBC website. In other places where relative humidity measurements are missing, we use a default of 85% over water and 70% over land. Where pressure measurements are missing, we use a default of 1013.25 mbar. Note that none of the CIMIS stations measure pressure. For the three non-ASOS ocean stations (NDBC-46012, NDBC-46026, and NDBC-pryc1) we use a salinity of 35 ppt, and for all other stations we use a salinity of 0 ppt. Note the COARE 3.6 algorithm is not as sensitive to air pressure or humidity as it is to air and water/soil temperatures, and it is barely sensitive at all to salinity, so we do not worry that these values are not perfect.

Some NDBC stations do not measure air temperature or water temperature, and sometimes temperature measurements are missing temporarily, so for each NDBC station we designate a "backup station" from which temperature data are pulled in the absence of primary station temperature data. The backup stations are listed in Table 5.

The final product of our wind processing is a collection of *.csv files containing hourly 10-m wind vectors, and a collection of netCDF (*.nc) files containing hourly auxiliary me-

Table 5: NDBC backup stations, used to fill in missing temperature data (air and water).

primary station	backup station
46012	46026
46026	46012
aamc1	rcmc1
dpxc1	pcoc1
ftpc1	prcy1
mzxc1	pcoc1
pcoc1	mzxc1
pryc1	ftpc1
psbc1	pcoc1
pxoc1	rcmc1
rcmc1	aamc1

terological data. These files are available in the **SFEI_Wind/Compiled_Hourly_10m_Winds/data** directory. Products are broken down by year. As an example, for 2013, the files **SFB_hourly_U10_2013.csv** and **SFB_hourly_V10_2013.csv** contain the 10-m hourly average wind vector components to the east and to the north, respectively, for all of 2013 and at all 52 wind observation stations, and the file **SFB_hourly_wind_and_met_data_2013.nc** contains hourly average auxiliary meterological data, including measured wind speeds, for all of 2013 and at all 52 wind observation stations. At this time, these products are available for years 2000-2017. As new wind data become available, we plan to add years 2018+.

Plots showing the complete hourly average meteorolgical record at each station and a comparison of hourly average measured wind speed with estimated 10-m wind speed at each station, for the 2000–2017 time window, are available in the **SFEI_Wind/Compiled_Hourly_10m_Winds/plots** directory. Figures 2 and 3 are two examples of the plots comparing measured wind speed with estimated 10-m wind speed. It is in general the case, as observed in these example figures, that the correction for atmospheric stability in stable conditions tends to make a bigger difference at the CIMIS (over-land) stations than at NDBC (over-water) stations. This is because air-soil temerature differences are often greater than air-water temperature differences.

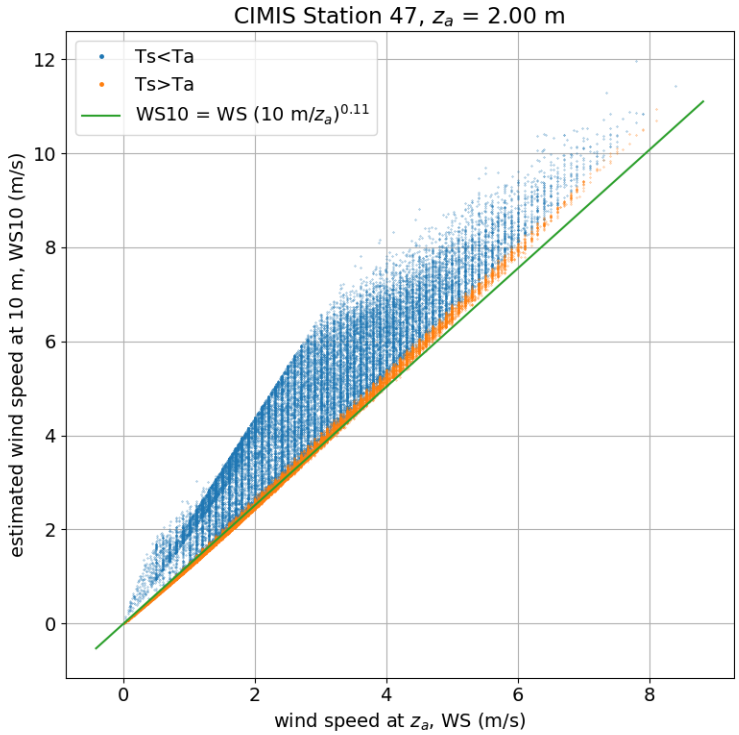

Figure 2: Comparison of wind speed measured at anemometer height $z_a = 2.0$ m and 10-m wind speed estimated using the modified COARE 3.6 algorithm for CIMIS Station 47, 2010-2017. Conditions where air temperature is greater than soil temperature ($T_a > T_s$) and vice-versa, approximately corresponding to stable and unstable conditions, respectively, are plotted in different colors. The 1/9 power law (often used for neutral conditions) is shown for comparison.

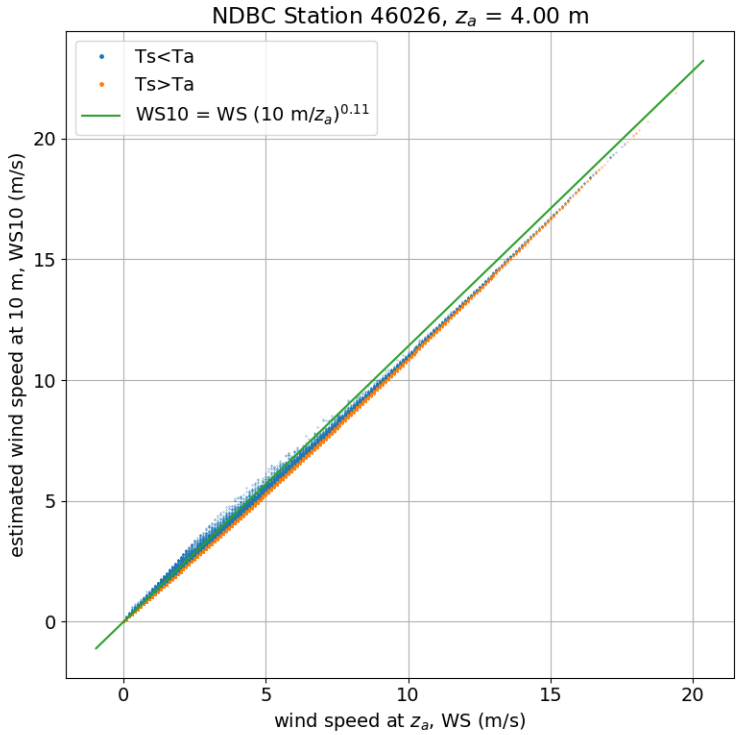

Figure 3: Comparison of wind speed measured at anemometer height $z_a = 4.0$ m and 10-m wind speed estimated using the modified COARE 3.6 algorithm for NDBC Station 46026, 2010-2017. Conditions where air temperature is greater than water temperature ($T_a > T_s$) and vice-versa, approximately corresponding to stable and unstable conditions, respectively, are plotted in different colors. The 1/9 power law (often used for neutral conditions) is shown for comparison.

4 Generating DFlow Wind Input Files from Observed Winds: Simple Interpolation Methods

As a simple alternative to the Ludwig wind model, we have written a Python script that interpolates hourly 10-m winds from the 52 stations around the SFB-Delta to obtain wind field inputs for DFlow (*.amu/*.amv files). At each hour, the script selects the stations that are reporting that hour and interpolates wind vector components from those stations onto the DFlow wind input grid. The user may select linear or natural neighbor interpolation and specify the extent and resolution for the grid. If linear interpolation is selected, the nearest neighbor method is used to extrapolate; the natural neighbor method automatically handles extrapolation. The script writes the interpolated/extrapolated hourly wind fields to the *.amu/*.amv files and also saves a plot showing what percentage of the time period each station was reporting. Percent reporting during WY2011, WY2013, and WY2016 is plotted in Figures 4, 5, and 6, respectively. Note that stations with zero percent reporting are plotted as dots for easy identification – some stations did not exist until 2014 or later, hence the complete lack of data from these stations in WY2011 and WY2013.

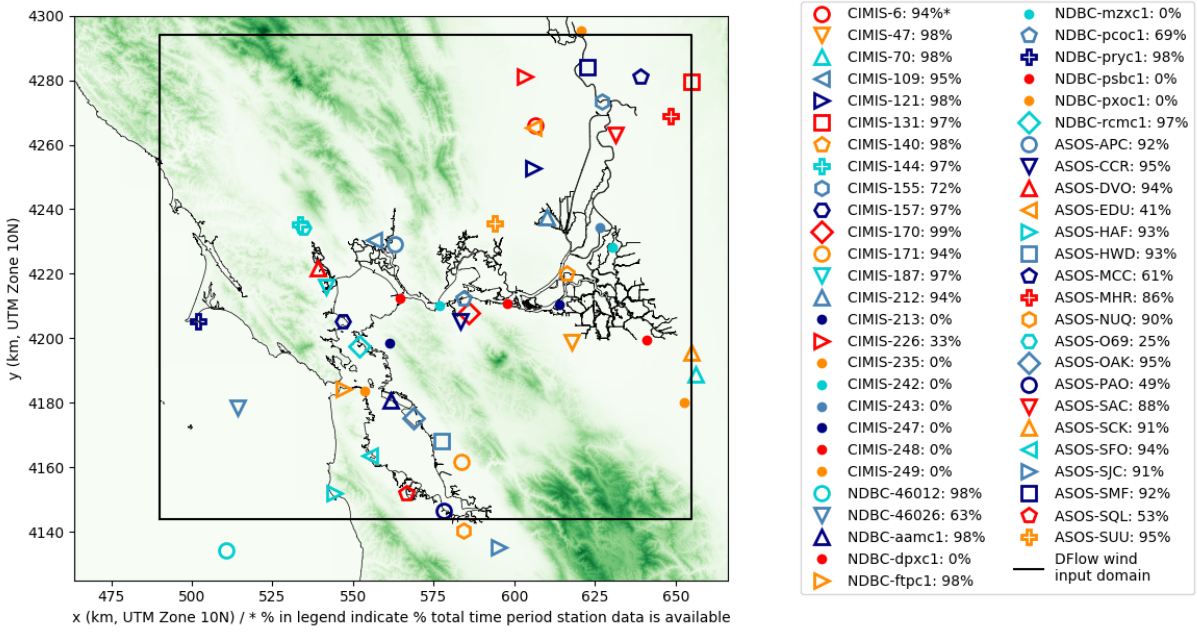

Figure 4: This map shows the percent of WY2011 each wind observation station was reporting.

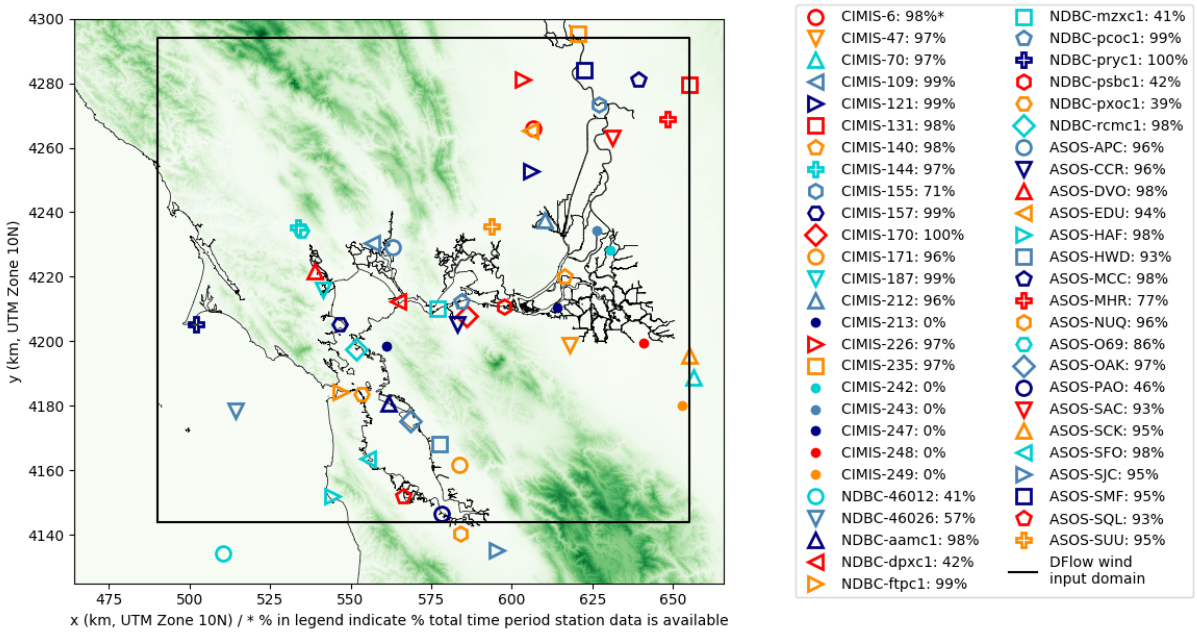

Figure 5: This map shows the percent of WY2013 each wind observation station was reporting.

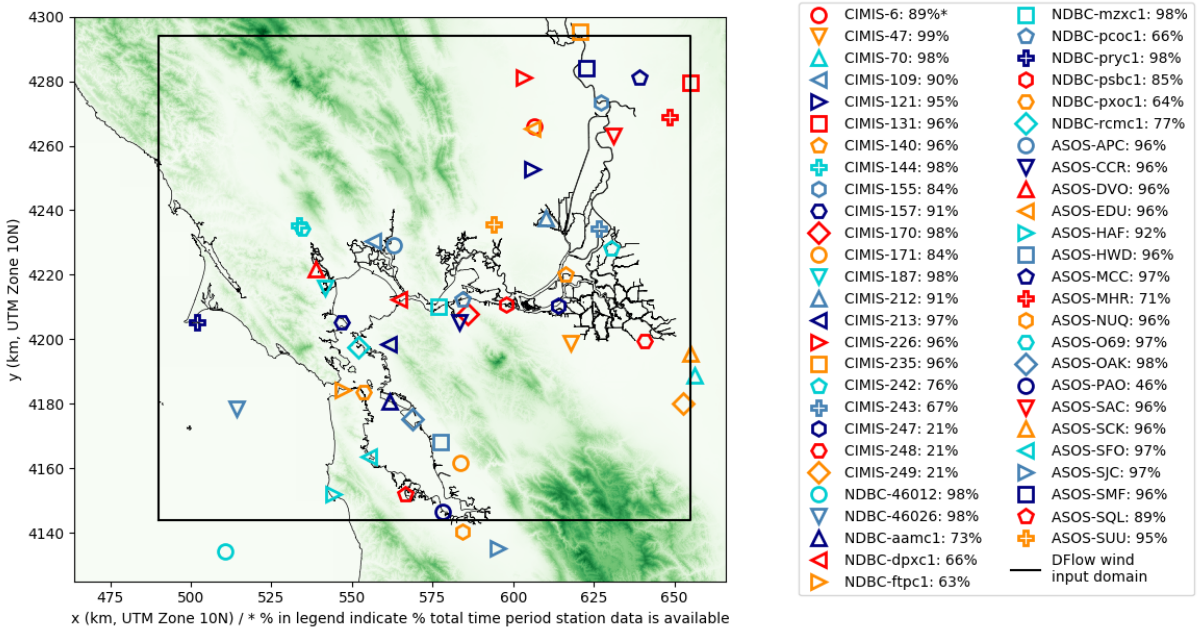

Figure 6: This map shows the percent of WY2016 each wind observation station was reporting.

5 Validation Studies

To validate the simple linear and natural neighbor interpolation methods, we systematically exclude one of the 47 wind observation stations inside the DFlow wind input grid domain at a time from the interpolation input data, comparing the interpolated winds at the location of the excluded station with the observed hourly 10-m winds at that station. To validate the Ludwig model, we use wind input files (*.amu/*.amv) generated by the Ludwig model, comparing hourly 10-m winds at each of the 47 observation stations inside the grid domain to winds at the grid point nearest that station in the *.amu/*.amv files. The WY2011 *.amu/*.amv files we test here were used as model input for the CASCaDE project WY2011 run (Martyr-Koller et al., 2017); the WY2013 *.amu/*.amv files we test here were used as model input for the SFEI Core Model WY2013 run (Nuss et al., 2018); and the WY2016 *.amu/*.amv files we test here were generated specifically for validation and have not been used as model input – these three sets of *.amu/*.amv files were generated using slightly different versions of the Ludwig model.

In addition to comparing hourly winds, we compare daily vector averages of modeled and observed winds. For each of the 47 stations, we identify times at which observations are available, and averaging over all of those times, we compute bias error and root mean square error (RMSE) for both wind speed and wind direction, and for both hourly and daily vector-averaged winds. Note that wind direction error is evaluated within the -180^o to 180^o window before averaging.

After evaluating bias error and RMSE for wind speed and direction at each of the 47 observation staitons inside the DFlow wind input domain, we take the average of these statistics across all stations (excluding stations from which no data are available). Average bias error is the mean absolute value of bias error across the stations, and average RMSE is the root mean square RMSE across the stations. The average bias error and RMSE are reported in Table 6 for hourly winds and in Table 7 for daily vector-averaged winds.

Performance of each model (Ludwig, linear interpolation, natural neighbor interpolation) is consistent across water years. Performance of linear and natural neighbor interpolation is very similar; both outperform the Ludwig model in all measures of validity. In both the hourly and daily wind statistics, bias error for wind speed is about the same for all models, but using linear or natural neighbor interpolation instead of the Ludwig model improves RMSE for wind speed by over 30% based on hourly winds and by $20-35\%$ based on daily vector-averaged winds. Both bias error and RMSE for wind direction are improved by using linear or natural neighbor interpolation instead of the Ludwig model: bias error is improved by around 50% based on both hourly winds and daily vector-averaged winds, and RMSE is

Table 6: Validation statistics for the Ludwig model, linear interpolation, and natural neighbor interpolation based on hourly winds. Statistics are computed at each station and then averaged across all 47 observation stations within the DFlow wind input domain, for various water years.

	Wind Speed (m/s)		Wind Direction (degrees)	
	bias	RMSE	bias	RMSE
WY2011: Ludwig model	1.0	2.8	15	84
WY2011: linear interpolation	0.9	1.9	7	60
WY2011: natural neighbor interpolation	0.9	1.9	7	60
WY2013: Ludwig model	0.9	2.8	16	77
WY2013: linear interpolation	0.9	1.9	9	58
WY2013: natural neighbor interpolation	0.9	1.9	9	57
WY2016: Ludwig model	1.0	2.8	19	79
WY2016: linear interpolation	0.9	1.8	9	57
WY2016: natural neighbor interpolation	0.9	1.8	9	55

Table 7: Validation statistics for the Ludwig model, linear interpolation, and natural neighbor interpolation based on daily vector-averaged winds. Statistics are computed at each station and then averaged across all 47 observation stations within the DFlow wind input domain, for various water years.

	Wind Speed (m/s)		Wind Direction (degrees)	
	bias	RMSE	bias	RMSE
WY2011: Ludwig model	0.8	2.0	21	70
WY2011: linear interpolation	0.8	1.3	8	40
WY2011: natural neighbor interpolation	0.8	1.4	8	42
WY2013: Ludwig model	0.8	1.8	19	54
WY2013: linear interpolation	0.8	1.4	11	36
WY2013: natural neighbor interpolation	0.8	1.5	10	37
WY2016: Ludwig model	0.8	1.8	25	60
WY2016: linear interpolation	0.8	1.3	11	37
WY2016: natural neighbor interpolation	0.7	1.3	11	37

improved by over 25% for hourly winds and over 30% for daily vector-averaged winds.

To give a sense of the detailed comparisons upon which validation statistics are based, let us consider an example. In Figures 7-13, we compare modeled and observed wind speed and direction via time series and scatter plots for WY2013 daily vector-averaged winds generated using (a) Ludwig, and (b) natural neighbor interpolation, at seven of the wind stations across the SFB-Delta. The seven stations are chosen to represent major subregions of the

SFB-Delta. Bias error and RMSE for a given station and wind model are reported on the appropriate scatter plot. Examining these plots, we see that neither wind estimation method is perfect, but natural neighbor interpolation outperforms the Ludwig model somewhat at most stations, and dramatically at the ocean station (NDBC 46026).

Similar time series and scatter plots comparing modeled and observed wind speed and direction at each of the 47 stations within the DFlow wind input domain, for both hourly and daily vector averages, for multiple water years, and for the three wind interpolation methods (Ludwig, linear, natural neighbor) are available in the **Validation_Studies** directory of the **SFEI_Wind** directory. There are far too many of these plots to include all of them here. Bias error and RMSE based on hourly and daily winds for each of the 47 stations within the DFlow wind input domain are also available, in *.csv files, in the **Validation_Studies** directory.

To visualize how bias error and RMSE vary across the SFB-Delta for the different interpolation methods, we use Pythyon's tricontourf function from the matplotlib library to generate contour plots from bias error and RMSE at the 47 observation stations. Contour plots of bias error and RMSE for wind speed and direction, computed from hourly winds, for all three interpolation methods (Ludwig, natural neighbor interpolation, linear interpolation), are shown in Figure 14 for WY2011, in Figure 15 for WY2013, and in Figure 16 for WY2016.

Figures 14-16 are similar to Figures 5-7 in Ludwig and Sinton (2000). If we compare Figure 5 in Ludwig and Sinton (2000) with our own Figures 14(a), 15(a), and 16(a), we see that our versions of the Ludwig model perform slightly better for wind speed but perform significantly worse for wind direction. It is possible that we are not running optimal versions of the Ludwig model, and some investment in tuning or debugging could result in better predictions.

Finally, let us examine yearly averages of the wind fields predicted by the three interpolation methods (technically, these are 14-month averages because of our definition of "water year"). In Figures 17, 18, and 19 we plot scalar mean wind speed, and the magnitude and direction of the mean wind vector for the three different interpolation methods for WY2011, WY2013, and WY2016, respectively, showing only the winds predicted over the hydrodynamic model domain, i.e., over the water. The mean wind fields from the linear and natural neighbor interpolation methods are very similar, but the natural neighbor method produces slightly smoother results, especially near the edges of the domain. Both linear and natural neighbor interpolation methods predict much higher wind speeds over the ocean compared to the Ludwig model. And where the Ludwig model predicts average wind direction predominantly to the east over the entire model domain, the natural neighbor and linear interpolation

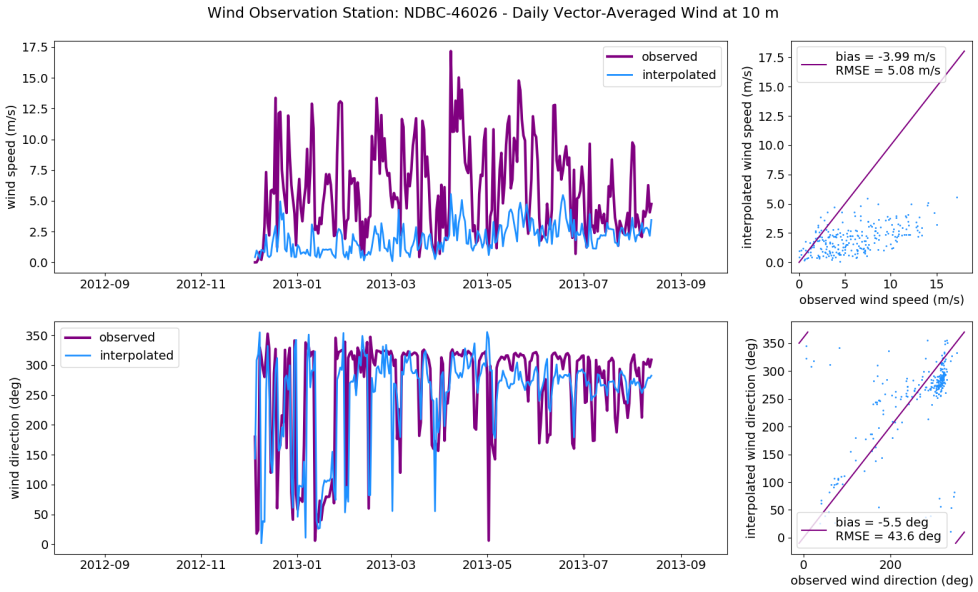

(a) Comparison of observed winds with winds from input files (*.amu/*.amv) used in the SFEI Core Model WY2013 simulation (Nuss et al., 2018). These wind input files were generated using the Ludwig model.

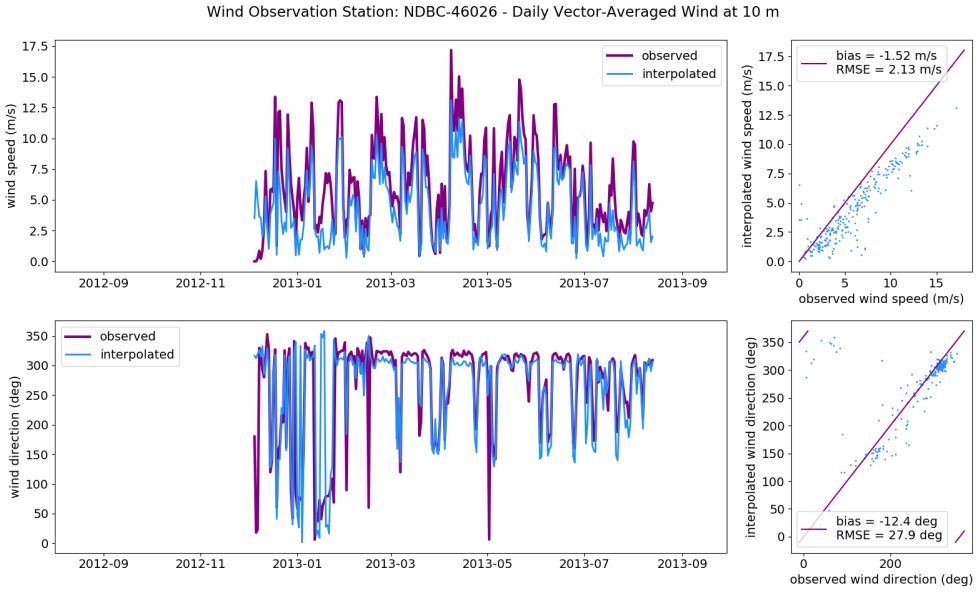

(b) Comparision of observed winds with winds predicted by natural neighbor interpolation.

Figure 7: Comparison of daily average wind vector magnitude and direction observed at NDBC Station 46026 (Pacific Ocean) with the daily average wind vector magnitude and direction estimated using (a) the Ludwig model, and (b) natural neighbor interpolation.

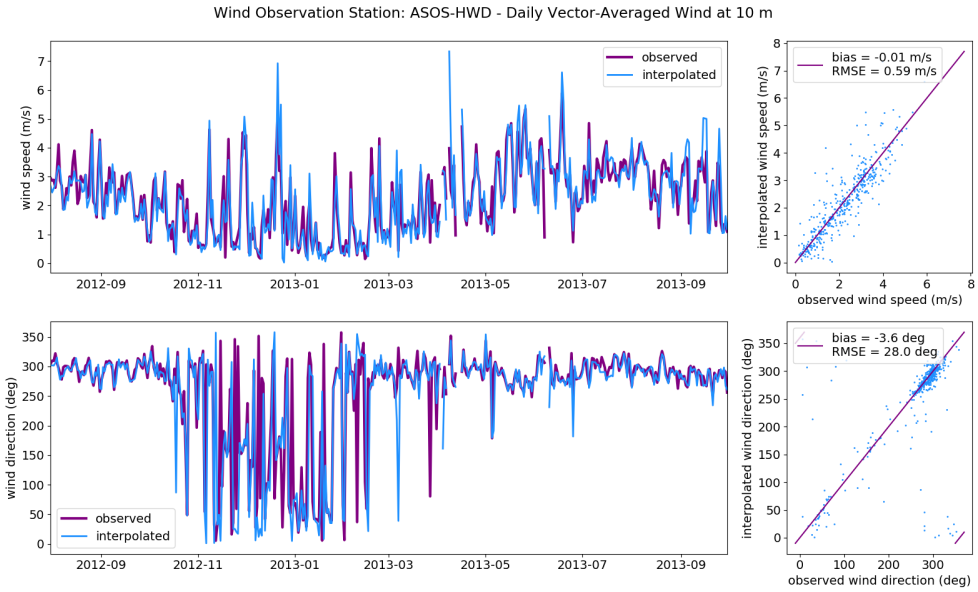

(a) Comparison of observed winds with winds from input files (*.amu/*.amv) used in the SFEI Core Model WY2013 simulation (Nuss et al., 2018). These wind input files were generated using the Ludwig model.

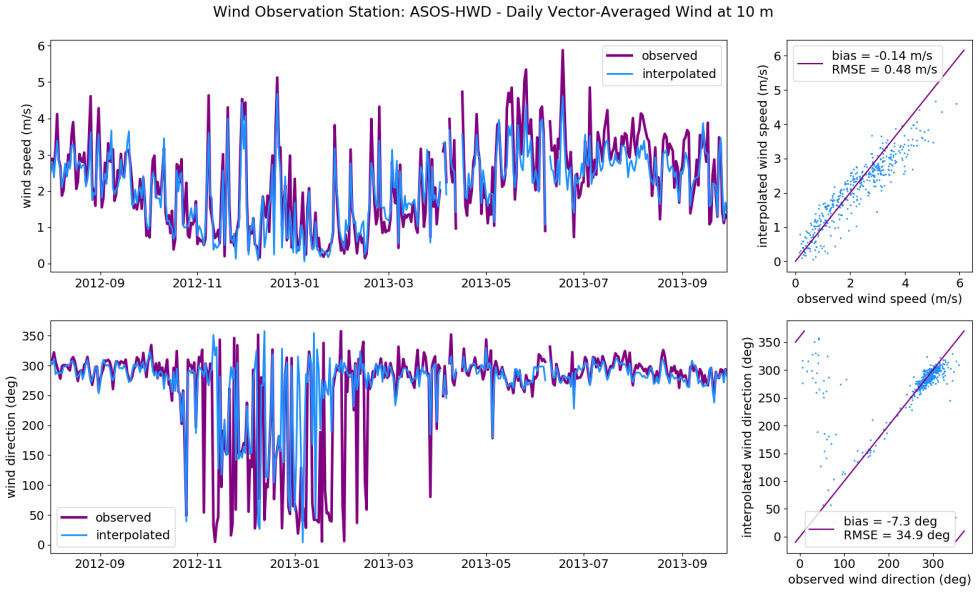

(b) Comparision of observed winds with winds predicted by natural neighbor interpolation.

Figure 8: Comparison of daily average wind vector magnitude and direction observed at ASOS Station HWD (South Bay) with the daily average wind vector magnitude and direction estimated using (a) the Ludwig model, and (b) natural neighbor interpolation.

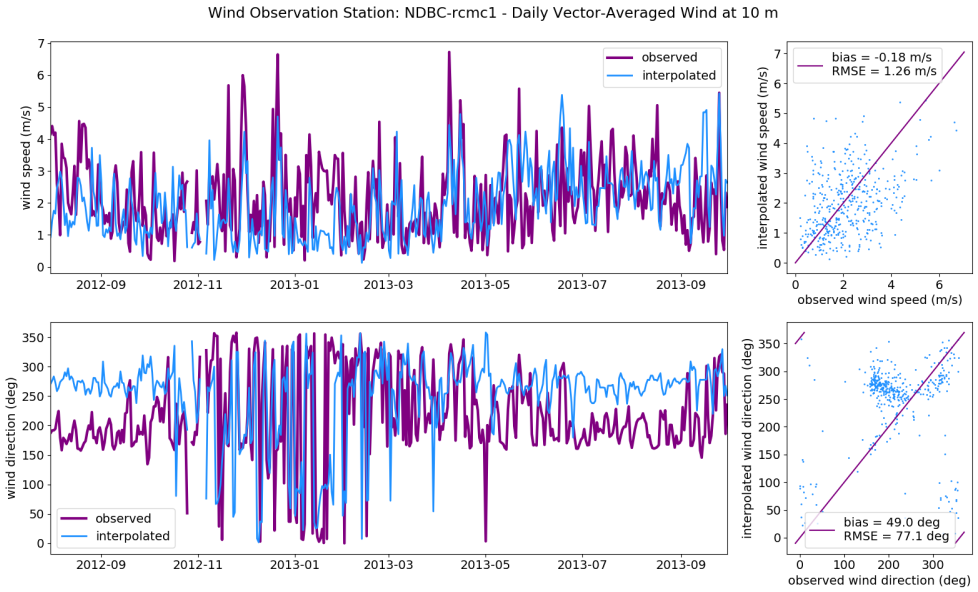

(a) Comparison of observed winds with winds from input files (*.amu/*.amv) used in the SFEI Core Model WY2013 simulation (Nuss et al., 2018). These wind input files were generated using the Ludwig model.

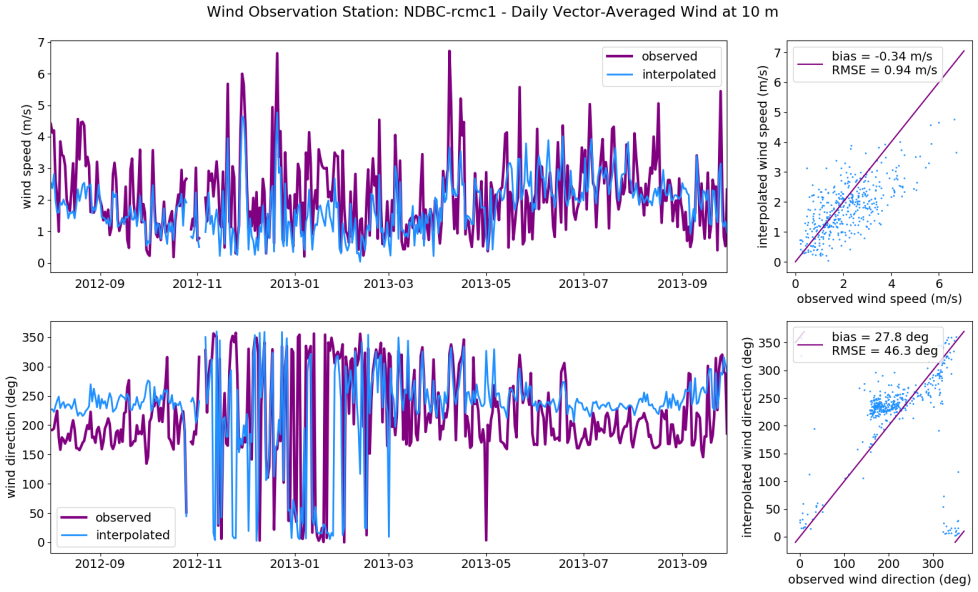

(b) Comparision of observed winds with winds predicted by natural neighbor interpolation.

Figure 9: Comparison of daily average wind vector magnitude and direction observed at NDBC Station rcmc1 (Central Bay) with the daily average wind vector magnitude and direction estimated using (a) the Ludwig model, and (b) natural neighbor interpolation.

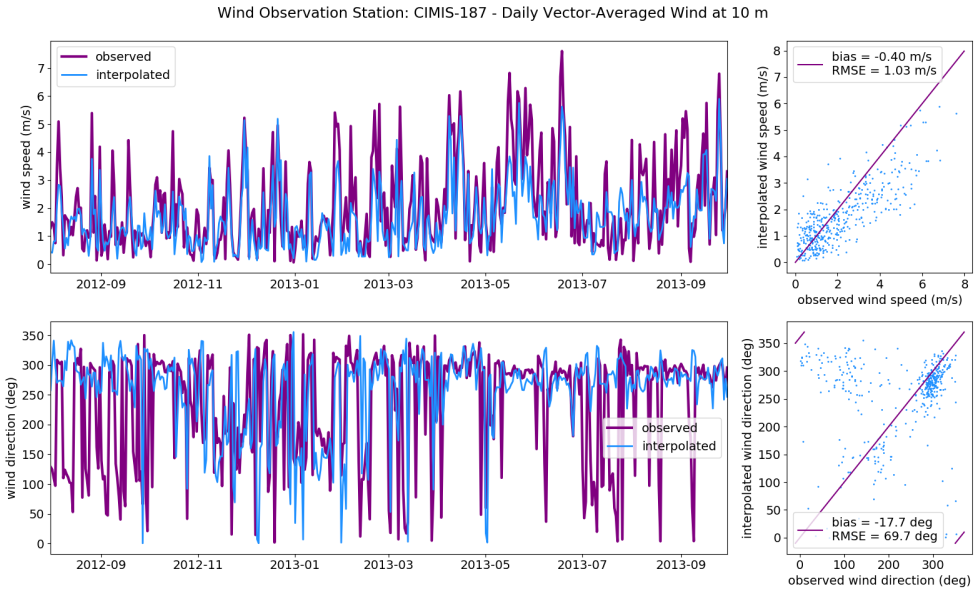

(a) Comparison of observed winds with winds from input files (*.amu/*.amv) used in the SFEI Core Model WY2013 simulation (Nuss et al., 2018). These wind input files were generated using the Ludwig model.

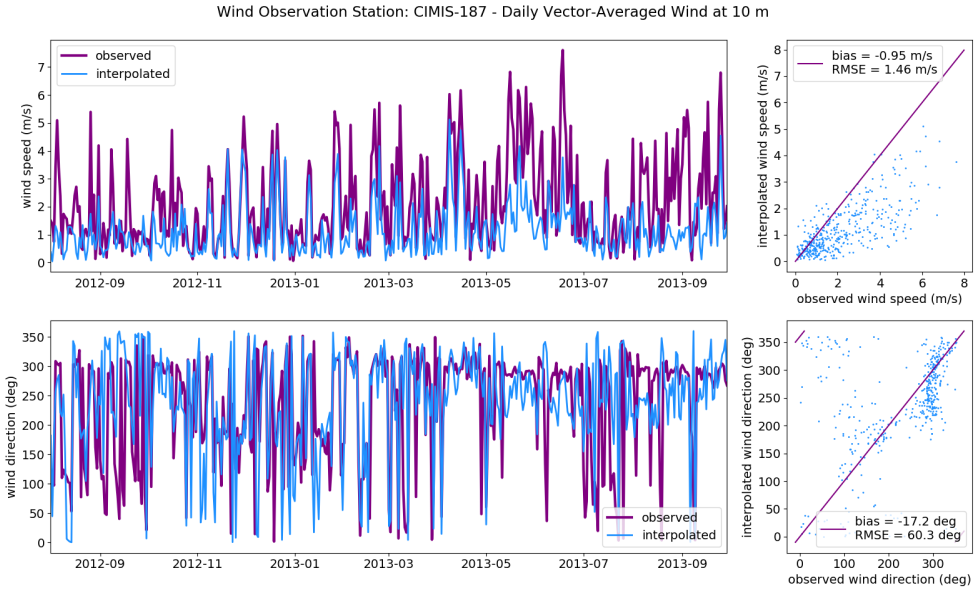

(b) Comparision of observed winds with winds predicted by natural neighbor interpolation.

Figure 10: Comparison of daily average wind vector magnitude and direction observed at CIMIS Station 187 (San Pablo Bay) with the daily average wind vector magnitude and direction estimated using (a) the Ludwig model, and (b) natural neighbor interpolation.

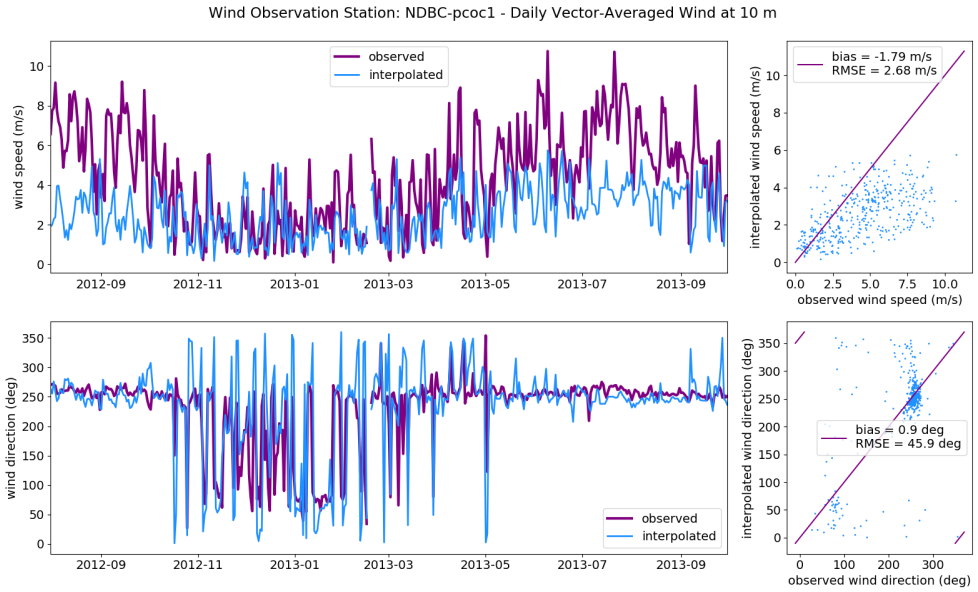

(a) Comparison of observed winds with winds from input files (*.amu/*.amv) used in the SFEI Core Model WY2013 simulation (Nuss et al., 2018). These wind input files were generated using the Ludwig model.

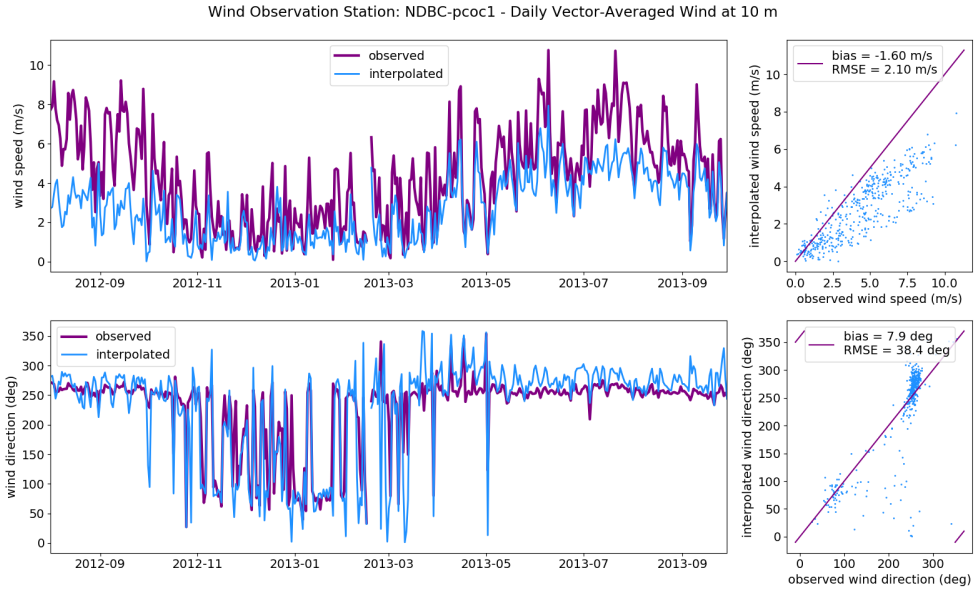

(b) Comparision of observed winds with winds predicted by natural neighbor interpolation.

Figure 11: Comparison of daily average wind vector magnitude and direction observed at NDBC Station pcoc1 (Suisun Bay) with the daily average wind vector magnitude and direction estimated using (a) the Ludwig model, and (b) natural neighbor interpolation.

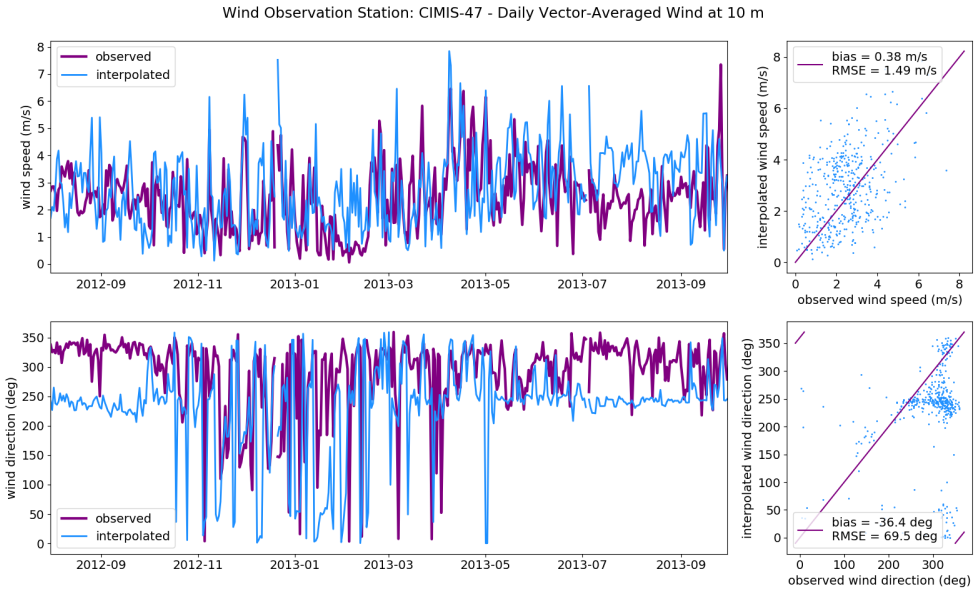

(a) Comparison of observed winds with winds from input files (*.amu/*.amv) used in the SFEI Core Model WY2013 simulation (Nuss et al., 2018). These wind input files were generated using the Ludwig model.

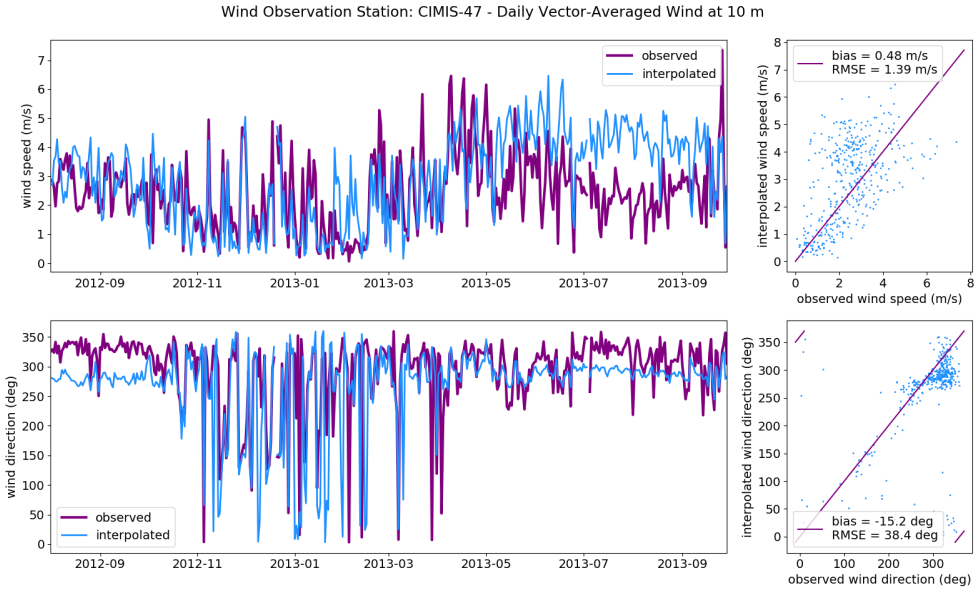

(b) Comparision of observed winds with winds predicted by natural neighbor interpolation.

Figure 12: Comparison of daily average wind vector magnitude and direction observed at CIMIS Station 47 (south Delta) with the daily average wind vector magnitude and direction estimated using (a) the Ludwig model, and (b) natural neighbor interpolation.

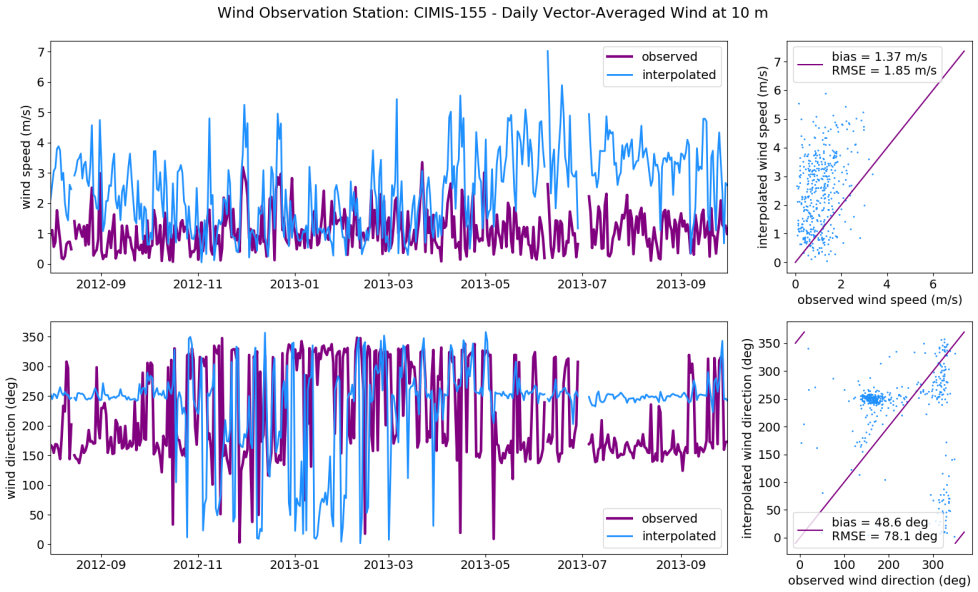

(a) Comparison of observed winds with winds from input files (*.amu/*.amv) used in the SFEI Core Model WY2013 simulation (Nuss et al., 2018). These wind input files were generated using the Ludwig model.

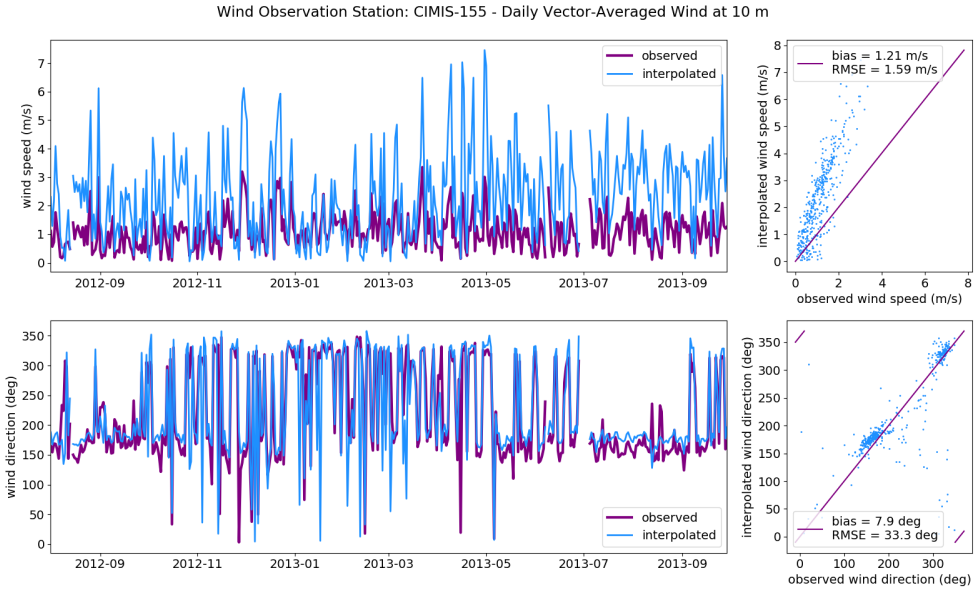

(b) Comparision of observed winds with winds predicted by natural neighbor interpolation.

Figure 13: Comparison of daily average wind vector magnitude and direction observed at CIMIS Station 155 (north Delta) with the daily average wind vector magnitude and direction estimated using (a) the Ludwig model, and (b) natural neighbor interpolation.

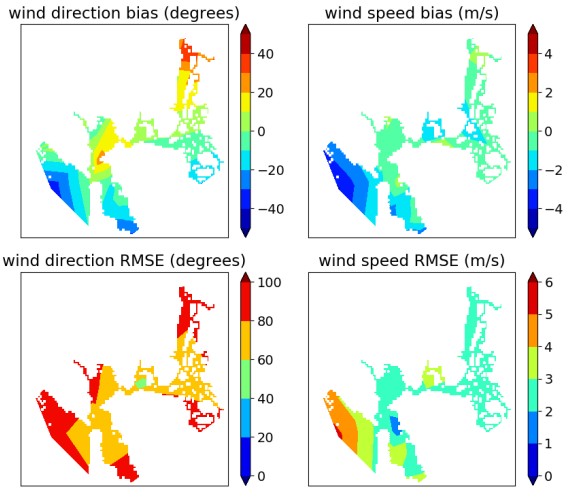

(a) Ludwig wind model.

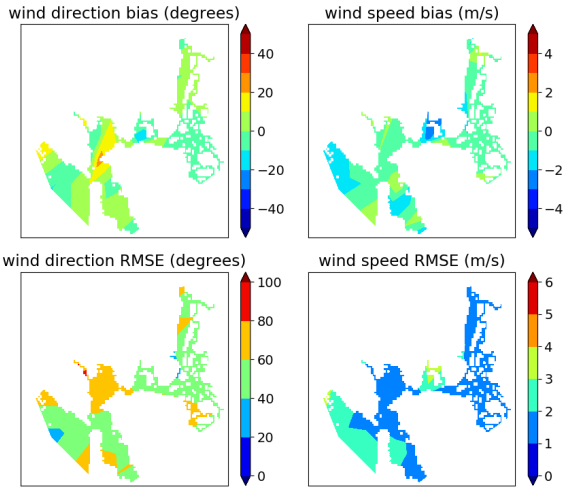

(b) Natural neighbor interpolation.

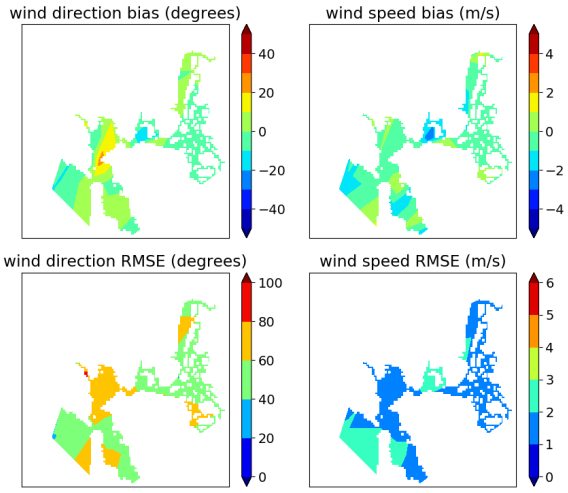

(c) Linear interpolation.

Figure 14: Hourly errors avereaged over WY2011 at the 47 observation stations within the DFlow wind input domain (excluding those with no data) are plotted using tricontourf.

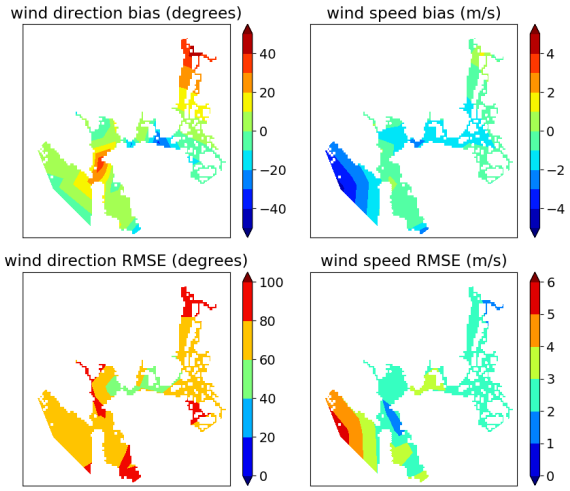

(a) Ludwig wind model.

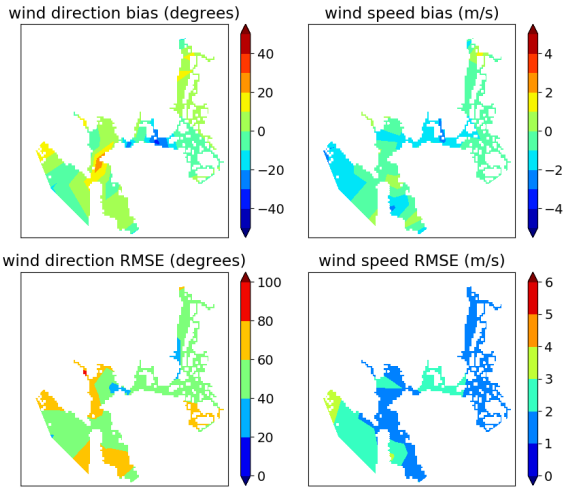

(b) Natural neighbor interpolation.

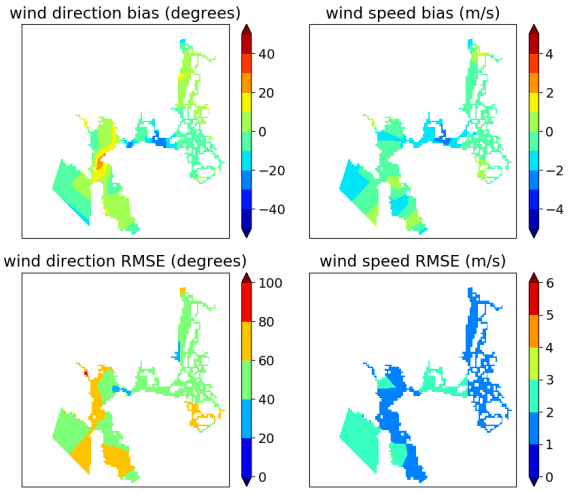

(c) Linear interpolation.

Figure 15: Hourly errors avereaged over WY2013 at the 47 observation stations within the DFlow wind input domain (excluding those with no data) are plotted using tricontourf.

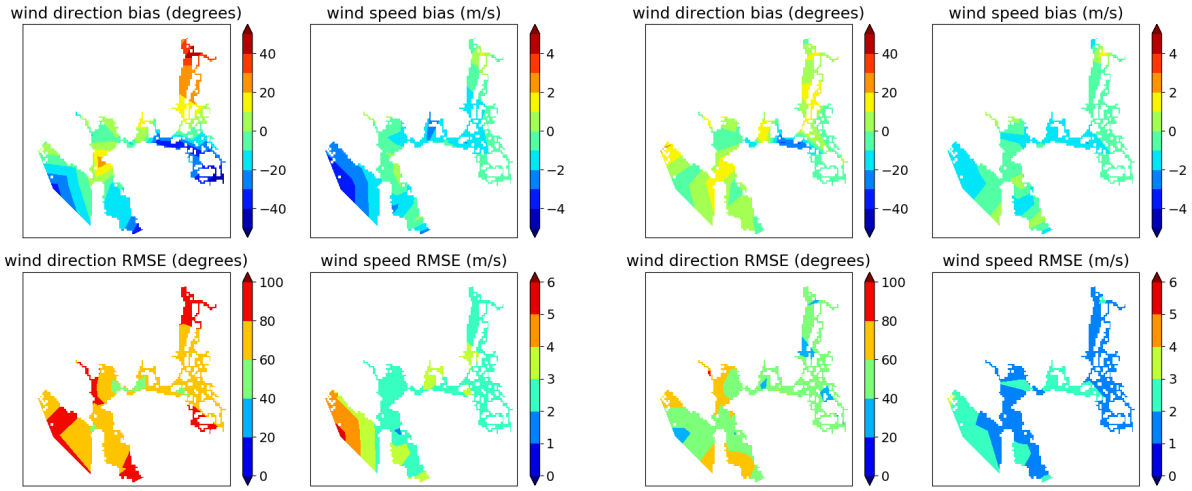

(a) Ludwig wind model.

(b) Natural neighbor interpolation.

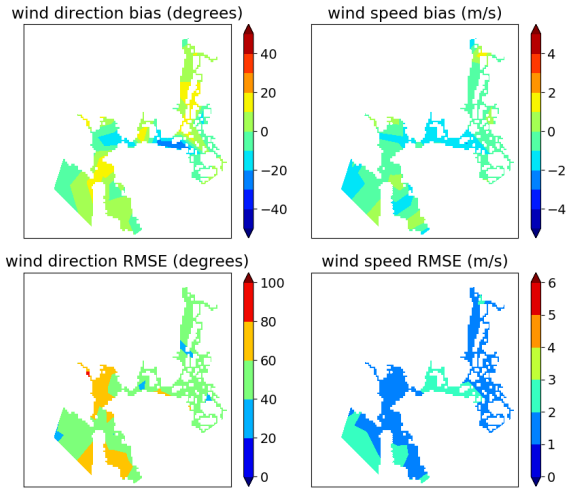

(c) Linear interpolation.

Figure 16: Hourly errors avereaged over WY2016 at the 47 observation stations within the DFlow wind input domain (excluding those with no data) are plotted using tricontourf.

methods predict winds to the southeast over the ocean veer east through the Golden Gate and then spread to the northeast and southeast as they fill the valleys where the Bay and Delta are located.

Figures 20-22 are the same as Figures 17-19 except that we show the average wind field over the entire 1.5 km x 1.5 m wind input grid, not just over the water. Here we see more differences between the linear and natural neighbor interpolation methods, and we clearly see that these methods (at least given the current 52 wind input stations) are not appropriate for predicting wind over land regions, except in the Delta, which is flat and surrounded by wind stations. If wind in the hills is of interest, the Ludwig model is still the best approach. This is partly because we excluded wind observation stations far from the water, but also because the Ludwig model accounts for terrain.

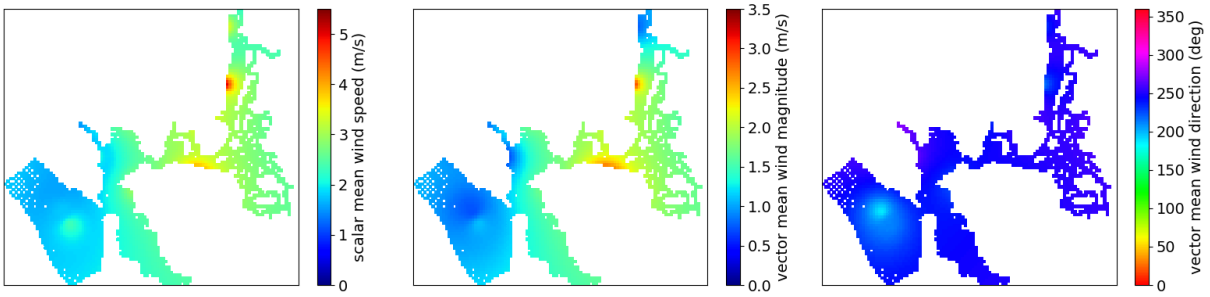

(a) Ludwig wind model.

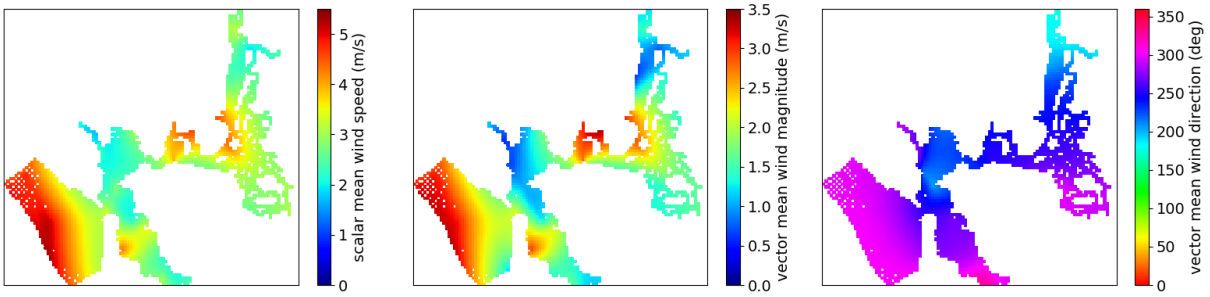

(b) Natural neighbor interpolation.

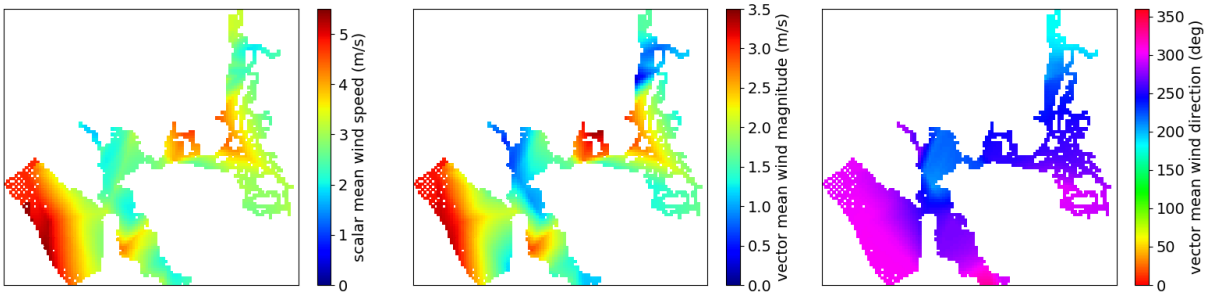

(c) Linear interpolation.

Figure 17: Wind field averaged over WY2011, as predicted by three different methods for interpolating onto the 1.5 km x 1.5 km DFlow wind input grid. Only winds over the hydrodynamic model domain are shown.

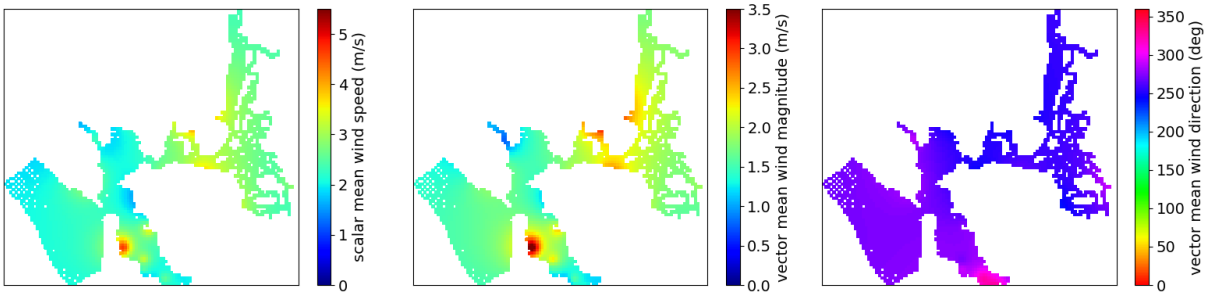

(a) Ludwig wind model.

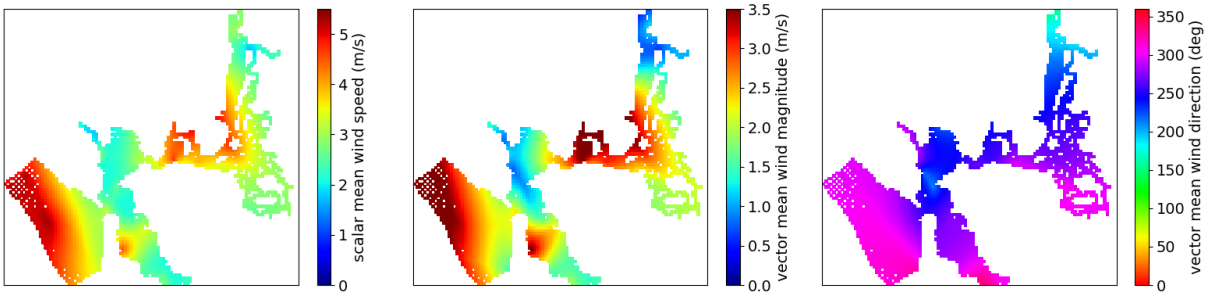

(b) Natural neighbor interpolation.

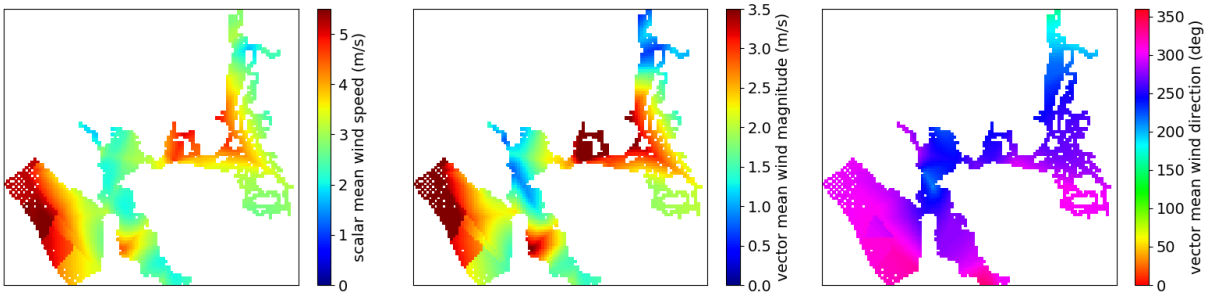

(c) Linear interpolation.

Figure 18: Wind field averaged over WY2013, as predicted by three different methods for interpolating onto the 1.5 km x 1.5 km DFlow wind input grid. Only winds over the hydrodynamic model domain are shown.

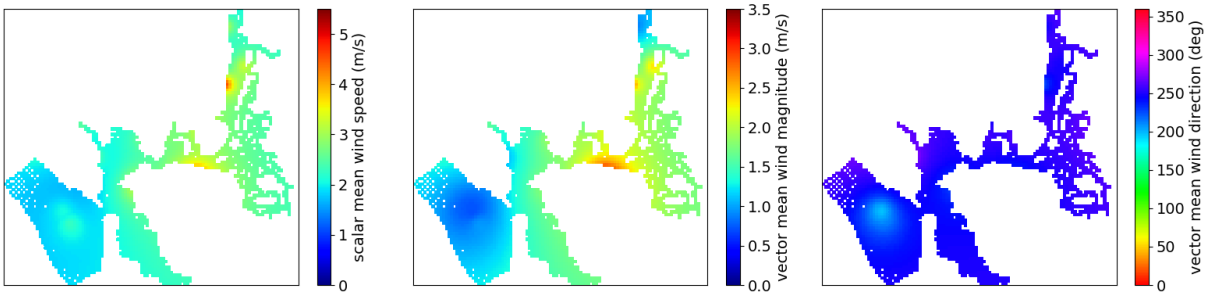

(a) Ludwig wind model.

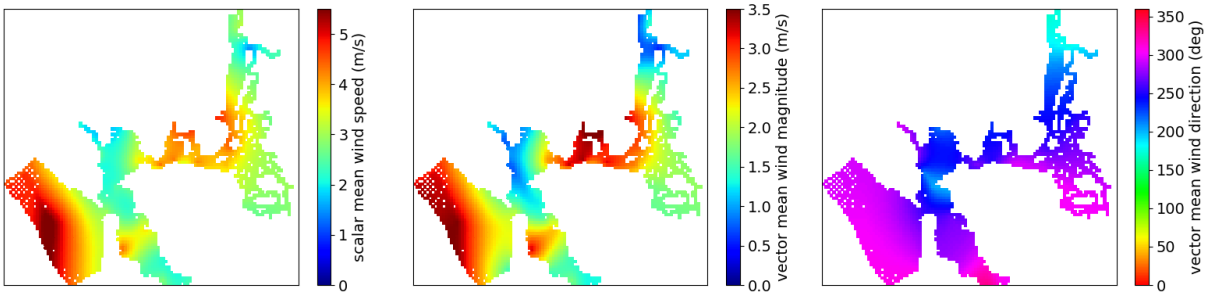

(b) Natural neighbor interpolation.

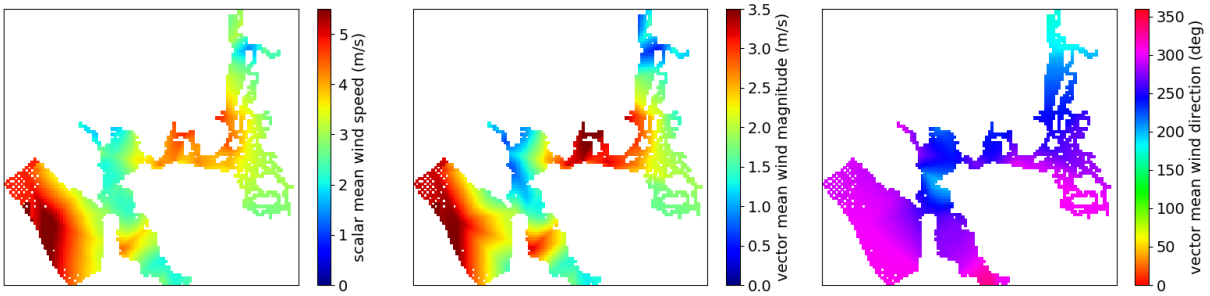

(c) Linear interpolation.

Figure 19: Wind field averaged over WY2016, as predicted by three different methods for interpolating onto the 1.5 km x 1.5 km DFlow wind input grid. Only winds over the hydrodynamic model domain are shown.

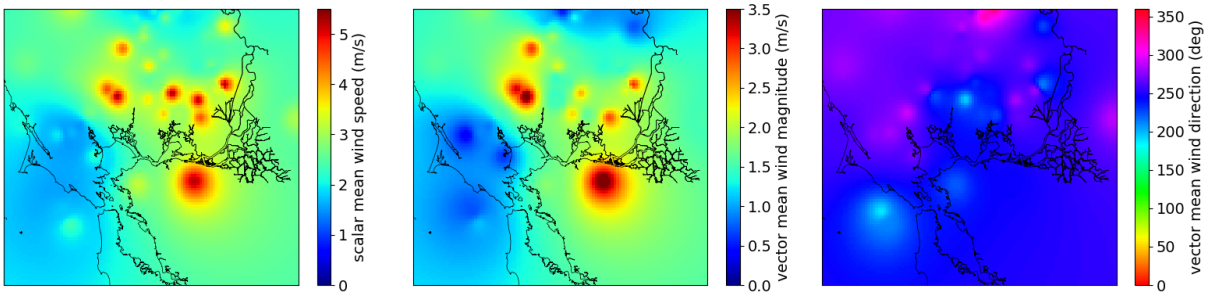

(a) Ludwig wind model.

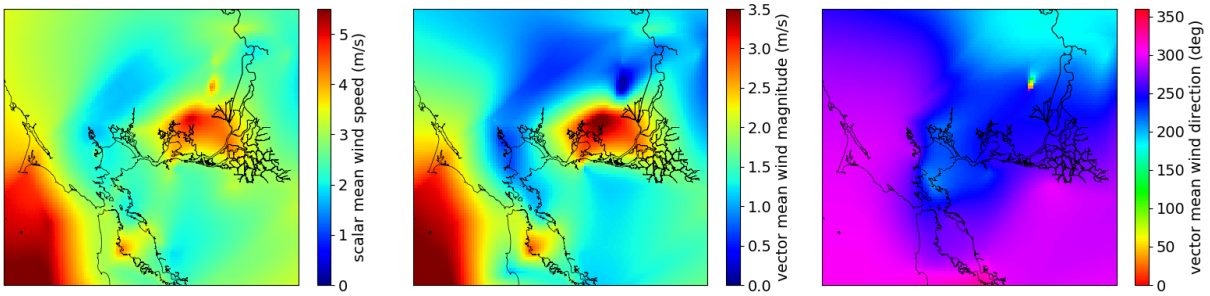

(b) Natural neighbor interpolation.

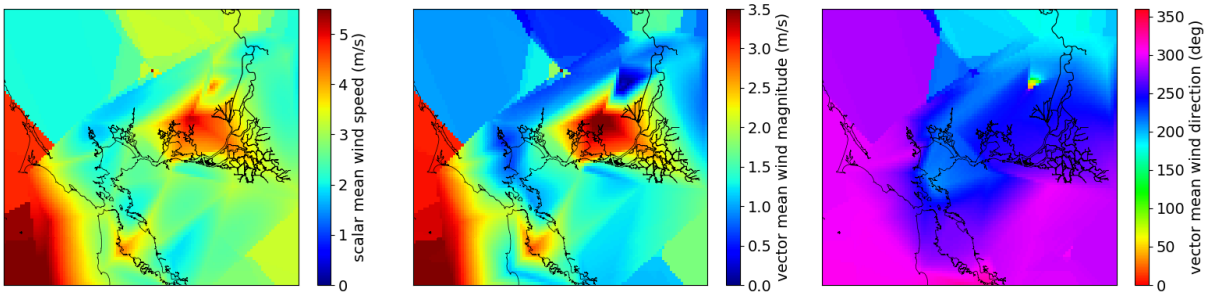

(c) Linear interpolation.

Figure 20: Wind field averaged over WY2011, as predicted by three different methods for interpolating onto the 1.5 km x 1.5 km DFlow wind input grid.

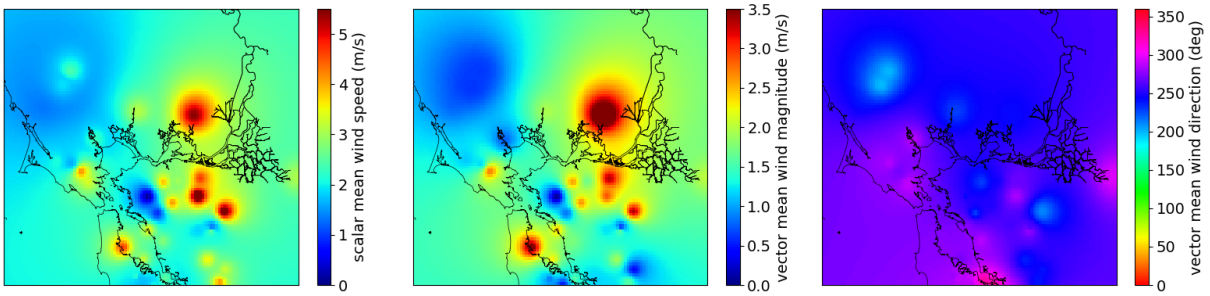

(a) Ludwig wind model.

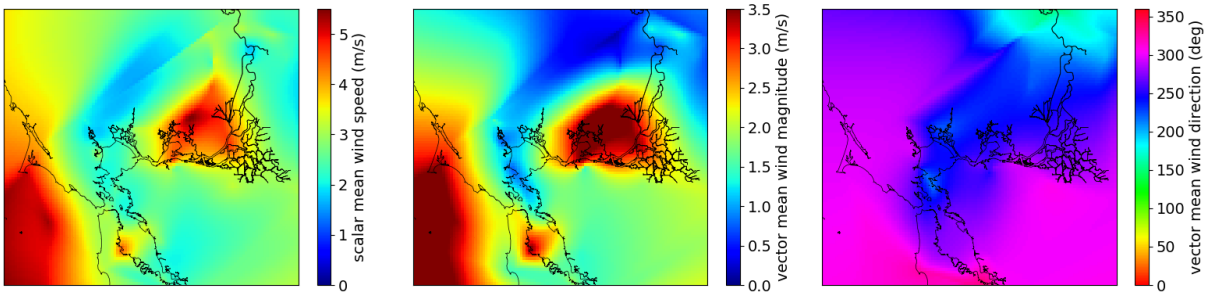

(b) Natural neighbor interpolation.

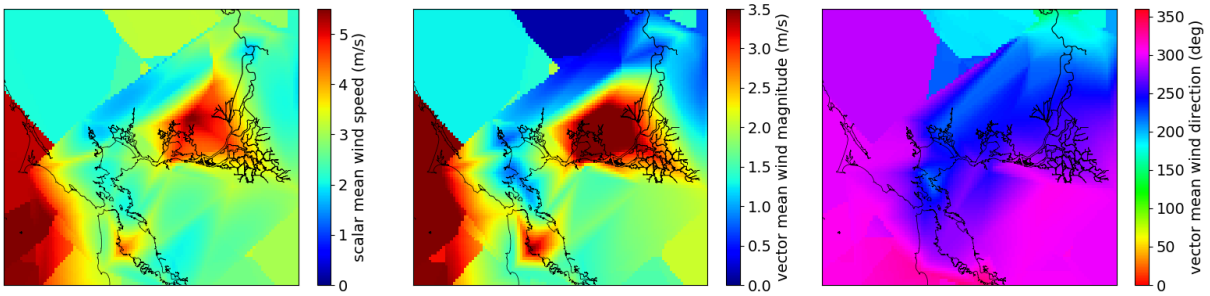

(c) Linear interpolation.

Figure 21: Wind field averaged over WY2013, as predicted by three different methods for interpolating onto the 1.5 km x 1.5 km DFlow wind input grid.

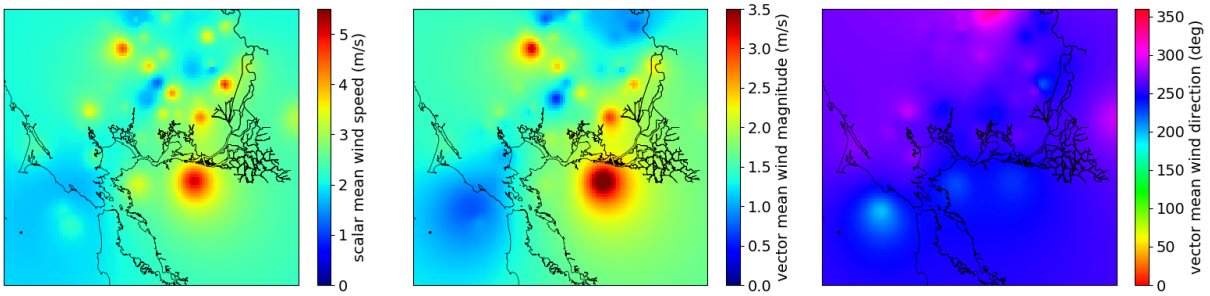

(a) Ludwig wind model.

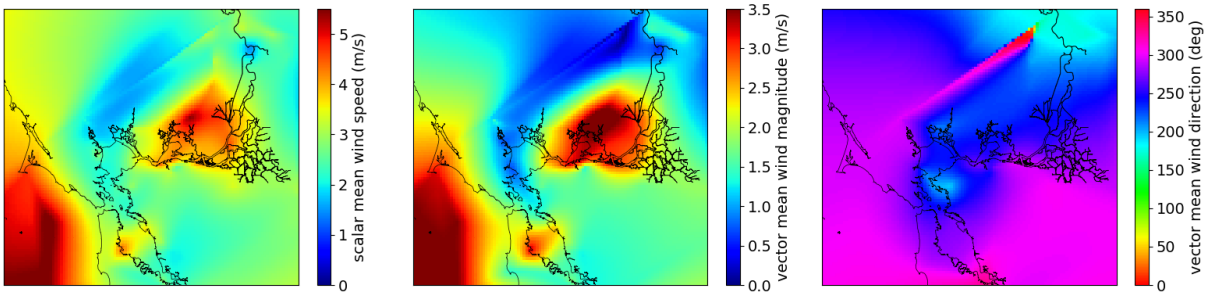

(b) Natural neighbor interpolation.

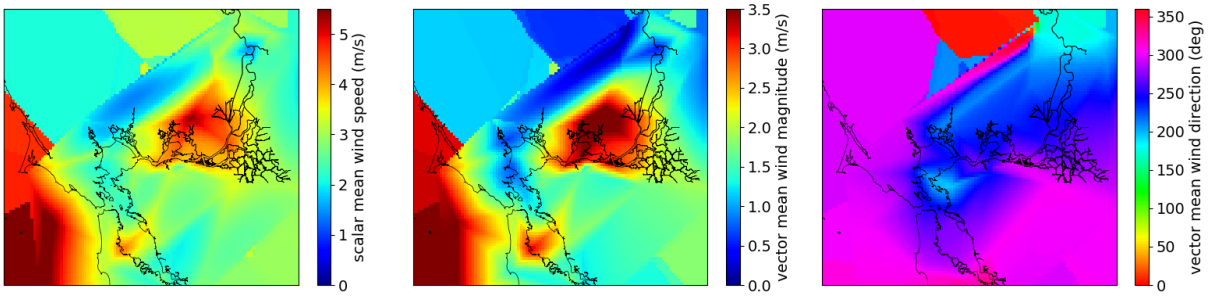

(c) Linear interpolation.

Figure 22: Wind field averaged over WY2016, as predicted by three different methods for interpolating onto the 1.5 km x 1.5 km DFlow wind input grid.

6 Conclusions

We have demonstrated that the Ludwig model (or at least the versions of the Ludwig model currently in the posession of Deltares, USGS, and SFEI) does not perform very well at most wind observations stations across the SFB-Delta and nearby coastal ocean. A simple linear or natural neighbor interpolation approach is about 30% more accurate than the Ludwig model for predicting wind speed. The improvent of accuracy is even greater for wind direction. We have developed the package **SFEI_Wind** to facilitate (1) consolidation of an hourly 10-m wind data set from observations at 52 stations across the Bay-Delta and nearby coastal ocean, and (2) easy generation of wind inputs for DFlow and other hydrodynamic models from this data set using linear or natural neighbor interpolation. The **SFEI_Wind** package is available on the SFEI Google Drive via the following link: **https://bit.ly/2U54rNZ**. Contact Allie King at **alliek@sfei.org** with questions.

The consolidated hourly observed 10-m wind data set for 2000-2017 is available in the **SFEI/Compiled_Hourly_10m_Winds/data** directory. DFlow wind input files (*.amu/ *.amv) generated by simple natural neighbor interpolation for water years 2001-2017 are available in the **SFEI_Wind/Wind4DFlow-SFB** directory. In this same directory are figures showing the percent reporting from each wind observation station for the time period represented in the corresponding *.amu/*.amv file. Please note that the wind fields in these *.amu/*amv files are more accurate for later years when more wind stations are in operation, especially in Central Bay and San Pablo Bay.

Our new approach to generating wind field inputs for SFB-Delta hydrodynamic models is not perfect. In the future, some improvements to **SFEI_Wind** could include:

1. Correction for the differences between wind measured over land and wind measured over water to yield better estimates of wind over water from land station observations.

2. Modification of the method for estimating surface roughness within COARE 3.6 to improve estimates in coastal and inland waters (the focus of the TOGA-COARE project was the tropical ocean).

3. Tricking hydrodynamic models into better estimaing wind stress from 10-m wind vectors by inputting the 10-m wind vectors that would have been measured in a neutral atmosphere given the observed stress (DFlow models presently estimate wind stress from wind vectors alone, without correcting for air and water temperature, typically assuming a neutral atmosphere). It would be simple to do this using the COARE 3.6 algorithm for stations over water, but it is less clear how to handle land stations, given that we are trying to estimate stress over water.

4. Estimating 10-minute-average winds from hourly-average winds, taking into account the different averaging periods and reporting frequencies at the different observation stations (see Section 2), using gust factors or some other approach (e.g. Harper et al., 2010).

5. Incorporating more sources of wind data, for example Bay Area Air Quality Management District data as in Bever et al. (2018). This would be especially helpful for earlier years when fewer stations in the CIMIS, NDBC, and ASOS networks were operating.

6. Adding years prior to 2000.

Collaborators are encouraged to make and share improvements to **SFEI_Wind**.

References

Achete, F. M., Wegen, M., Roelvink, D., and Jaffe, B. (2015). A 2-D process-based model for suspended sediment dynamics: a first step towards ecological modeling. *Hydrology and Earth System Sciences*, 19:2837–2857.

Bever, A. J., MacWilliams, M. L., and Fullerton, D. K. (2018). Influence of an observed decadal decline in wind speed on turbidity in the san francisco estuary. *Estuaries and Coasts*, 41:1943–1967.

Brutsaert, W. (1982). *Evaporation in the Atmosphere: Theory, History and Applications*. Retrieved from https://www.springer.com/us/book/9789027712479.

Deltares (2019). *D-Flow Flexible Mesh User Manual*. [Draft]. Delft3D FM Suite 2019.1, March 22, 2019.

Fairall, C., Blomquist, B., Bariteau, L., and Edson, J. (2018). *The TOGA-COARE Bulk Air-Sea Flux Algorithm*. [Software, Version 3.6]. Retrieved from ftp://ftp1.esrl.noaa.gov/BLO/Air-Sea/bulkalg/cor3_6/.

Harper, B. A., Kepert, J. D., and Ginger, J. D. (2010). Guidelines for converting between various wind averaging periods in tropical cyclone conditions. Technical report, World Meteorological Organization, Geneva, Switzerland.

Hignett, P. (1994). Roughness lengths for temperature and momentum over heterogeneous terrain. *Boundary-Layer Meteorology*, 68:225–236.

Ludwig, F. L., Livingston, J. M., and Endlich, R. M. (1991). Use of mass conservation and critical dividing streamline concepts for efficient objective analysis of winds in complex terrain. *J. Appl. Meteor.*, 30:1490–1499.

Ludwig, F. L. and Sinton, D. (2000). Evaluating an objective wind analysis technique with a long record of routinely collected data. *J. Appl. Meteor.*, 39:335–348.

Martyr-Koller, R. C., Kernkamp, H. W. J., van Dam, A., van der Wegen, M., Lucas, L. V., Knowles, N., Jaffe, B., and Fregoso, T. A. (2017). Application of an unstructured 3D finite volume numerical model to flows and salinity dynamics in the San Francisco Bay-Delta. *Estuarine, Coastal and Shelf Science*, 192:86–107.

Nuss, E., Zhang, Z., Holleman, R., Chelsky, A., Winchell, T., Wu, J., and Senn, D. (2018). Hydrodynamic and water quality model calibration and application in San Francisco Bay.

Technical report, San Francisco Estuary Institute, Richmond, CA. SFEI Contribution No. 913.

SFB 90-m DEM (2011). Digital Elevation Model (90m): San Francisco Bay Area, California. Retrieved from https://earthworks.stanford.edu/catalog/stanford-vq725mh7108.